2369-19

CIMPA/ICTP Geometric Structures and Theory of Control

1 - 12 October 2012

Hall-MHD and applications (part II)

Daniel Gomez

IAFE, Buenos Aires
Argentina

Hall – MHD

and applications (part II)

Daniel Gómez [1,2]

Email: dgomez@df.uba.ar Webpage: http://astro.df.uba.ar

(1) Instituto de Astronomia y Fisica del Espacio, CONICET, Argentina
(2) Departamento de Fisica, Universidad de Buenos Aires, Argentina

Joint ICTP-IAEA College on Plasma Physics, Abdus Salam ICTP, October 11, 2012

Hall-MHD equations

- The dimensionless version, for a length scale L_0, density n_0 and Alfven speed $v_A = B_0 / \sqrt{4\pi m_i n_0}$

$$\frac{d\vec{U}}{dt} = \frac{1}{\varepsilon}(\vec{E} + \vec{U} \times \vec{B}) \quad - \frac{\beta}{n}\vec{\nabla} p_i - \frac{\eta}{\varepsilon n}\vec{J} + \nu \nabla^2 \vec{U} \qquad \nu = \frac{\mu}{m_i n v_A L_0}$$

$$0 = -\frac{1}{\varepsilon}(\vec{E} + \vec{U}_e \times \vec{B}) - \frac{\beta}{n}\vec{\nabla} p_e + \frac{\eta}{\varepsilon n}\vec{J} \qquad \text{where} \qquad \vec{J} = \vec{\nabla} \times \vec{B} = \frac{n}{\varepsilon}(\vec{U} - \vec{U}_e)$$

- We define the Hall parameter $\varepsilon = \frac{c}{\omega_{pi} L_0}$

  as well as the plasma *beta* $\beta = \frac{p_0}{m_i n_0 v_A^2}$ and the electric resistivity $\eta = \frac{c^2 \nu_{ie}}{\omega_{pi}^2 L_0 v_A}$

- Adding these two equations yields:

$$\boxed{n\frac{d\vec{U}}{dt} = (\vec{\nabla} \times \vec{B}) \times \vec{B} - \beta \vec{\nabla}(p_i + p_e) + \nu \nabla^2 \vec{U}}$$

Hall-MHD equations

- On the other hand, using

$$\left.\begin{aligned} \vec{E} &= -\frac{1}{c}\frac{\partial \vec{A}}{\partial t} - \vec{\nabla}\phi \\ \vec{B} &= \vec{\nabla} \times \vec{A} \end{aligned}\right\} \rightarrow \boxed{\frac{\partial \vec{A}}{\partial t} = (\vec{U} - \frac{\varepsilon}{n}\vec{\nabla} \times \vec{B}) \times \vec{B} - \vec{\nabla}\phi + \frac{\varepsilon\beta}{n}\vec{\nabla} p_e - \frac{\eta}{n}\vec{\nabla} \times \vec{B}}$$

Hall MHD in a strong field

- The RHMHD equations are (Gomez, Dmitruk & Mahajan 2008):

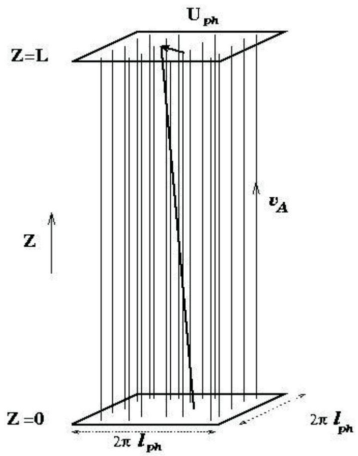

$$\boxed{\begin{aligned}
\partial_t a &= \partial_z(\varphi-\varepsilon b)+[\varphi-\varepsilon b, a] && +\eta\nabla_\perp^2 a\\
\partial_t \omega &= \partial_z j \qquad +[\varphi,\omega]-[a, j] && +\nu\nabla_\perp^2 \omega\\
\partial_t b &= \partial_z(u-\varepsilon j) \ +[\varphi, b]+[u-\varepsilon j, a] && +\eta\nabla_\perp^2 b\\
\partial_t u &= \partial_z b \qquad +[\varphi, u]-[a, b] && +\nu\nabla_\perp^2 u
\end{aligned}}$$

where

$$\vec{B}=\hat{z}+\vec{\nabla}\times(a\hat{z}+g\hat{x})=[a_y,-a_x,1+b] \quad , \quad b=-g_y$$

$$\vec{U}=\vec{\nabla}\psi+\vec{\nabla}\times(\varphi\,\hat{z}+f\,\hat{x})=[\varphi_y+\psi_x,-\varphi_x+\psi_y,u+\psi_z] \quad , \quad u=-f_y$$

- These are the RHMHD equations. Their ideal invariants (just as for 3D HMHD) are:

$$E=\frac{1}{2}\int d^3r(|\vec{U}|^2+|\vec{B}|^2)=\frac{1}{2}\int d^3r(|\vec{\nabla}_\perp\varphi|^2+|\vec{\nabla}_\perp a|^2+u^2+b^2) \qquad \text{energy}$$

$$H_m=\frac{1}{2}\int d^3r(\vec{A}\cdot\vec{B})=\int d^3r\, ab \qquad \text{magnetic helicity}$$

$$H_h=\frac{1}{2}\int d^3r(\vec{A}+\varepsilon\vec{U})\cdot(\vec{B}+\varepsilon\vec{\Omega})=\int d^3r(ab+\varepsilon(a\omega+ub)+\varepsilon^2 u\omega) \qquad \text{hybrid helicity}$$

Linear modes of the RHMHD equations

- Retaining the linear terms in the RHMHD eqs we obtain the following dispersion relationship

$$\omega^4 - 2k_z^2\left(1+\frac{(\varepsilon k_\perp)^2}{2}\right)\omega^2 + k_z^4 = 0$$

which displays the following (dispersive) modes

$$\omega_\pm = \sqrt{k_z^2 + \left(\frac{\varepsilon k_\perp k_z}{2}\right)^2} \pm \frac{\varepsilon k_\perp k_z}{2}$$

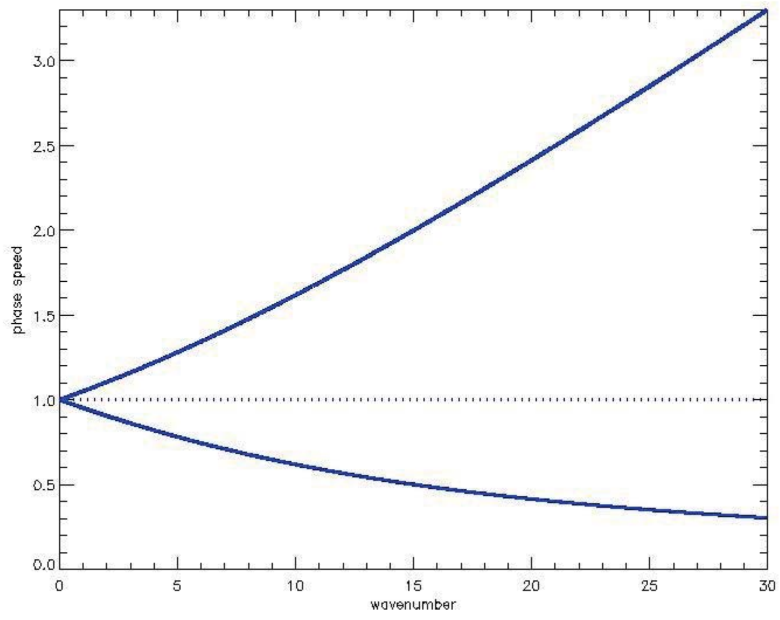

- The positive branch corresponds to (right hand, circularly polarized) *whistlers*, while the negative branch are (left hand polarized) *ion-cyclotron* waves.

- The phase speed for *whistlers* grows like $c_+ \approx \varepsilon k_\perp$ thus forcing to a very small dt for numerical convergence.

- *Ion-cyclotron* waves, instead, display a decreasing phase speed like $c_- \approx 1/\varepsilon k_\perp$, which makes them good candidates for resonant particle acceleration.

Hall-MHD reconnection in 2.5D

- Hall reconnection has extensively been studied for the Earth's magnetopause and also the magnetotail. The Hall effect is expected to increase the reconnection rate.

- The simplest geometrical setup is 2.5D, for which the velocity and magnetic field can be written in terms of four scalar fields (Gómez 2006, Space Sci. Rev. 122, 231; Gómez et al. 2006, Adv. Sp. Res. 37, 1287)

$$\vec{B}(x,y,t) = \vec{\nabla}\times\left[\hat{z}\,a(x,y,t)\right] + \hat{z}\,b(x,y,t)$$

$$\vec{U}(x,y,t) = \vec{\nabla}\times\left[\hat{z}\,\phi(x,y,t)\right] + \hat{z}\,u(x,y,t)$$

$$\vec{U}_e = \vec{U} - \varepsilon\,\vec{J} = \vec{\nabla}\times\left[\hat{z}(\phi-\varepsilon\,b)\right] + \hat{z}(u-\varepsilon\,j)$$

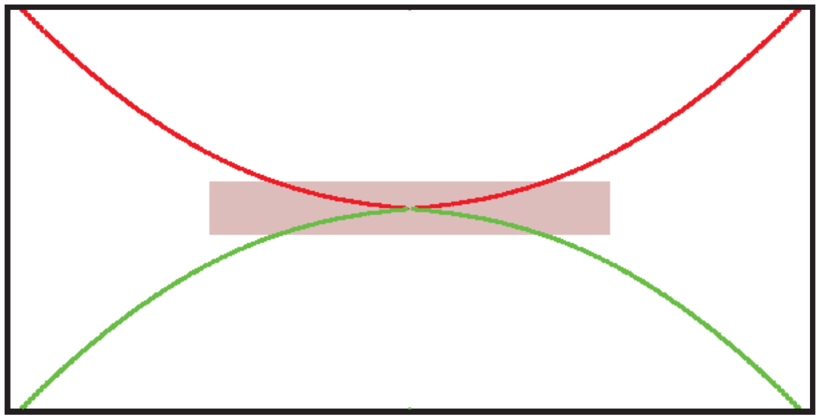

- The 2.5D Hall-MHD equations are

$$\partial_t a = [\phi-\varepsilon\,b, a] + \eta\nabla^2 a$$

$$\partial_t \omega = [\phi,\omega] + [j,a] + \nu\nabla^2\omega$$

$$\partial_t b = [\phi,b] + [u-\varepsilon\,j, a] + \eta\nabla^2 b$$

$$\partial_t u = [b,a] + [\phi,u] + \nu\nabla^2 u$$

where $\omega = -\nabla^2\phi \quad , \quad j = -\nabla^2 a$

- In the absence of Hall , the parallel components (u,b) have no influence on the perp. dynamics.

- When Hall is present, the parallel components will be turned on and couple to the perp. components.

Hall-MHD reconnection in 2D

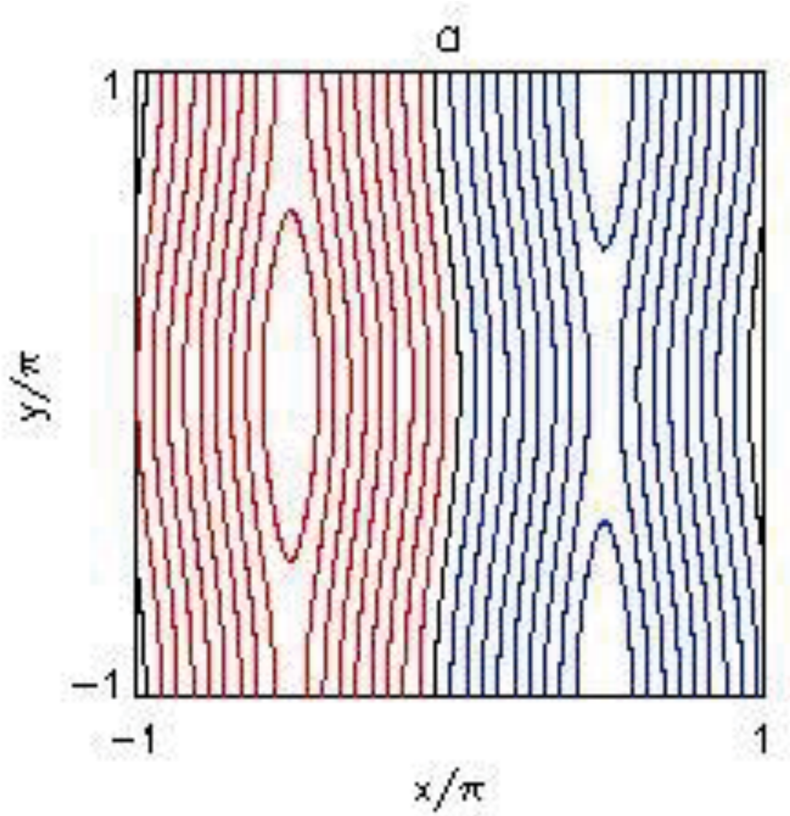

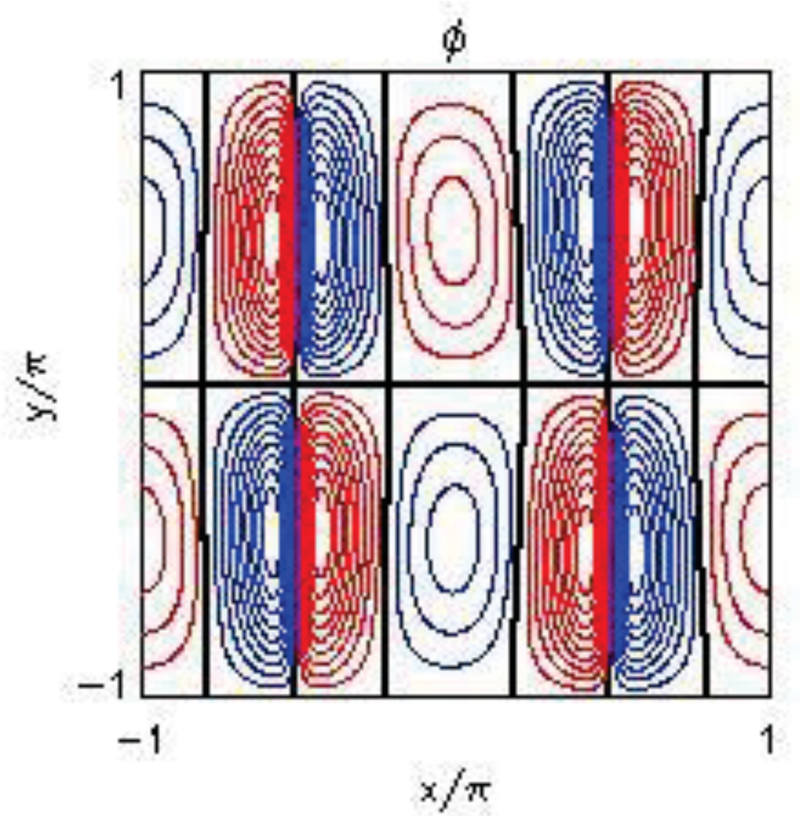

- When the Hall effect is neglected (pure MHD) **2D** reconnection is possible.

- Magnetic **fieldlines** (left) and flow **streamlines** (right) are shown at three succesive Alfven times. **Blue** contours are **positive** and the **red** ones are **negative**.

Hall-MHD reconnection in 2D

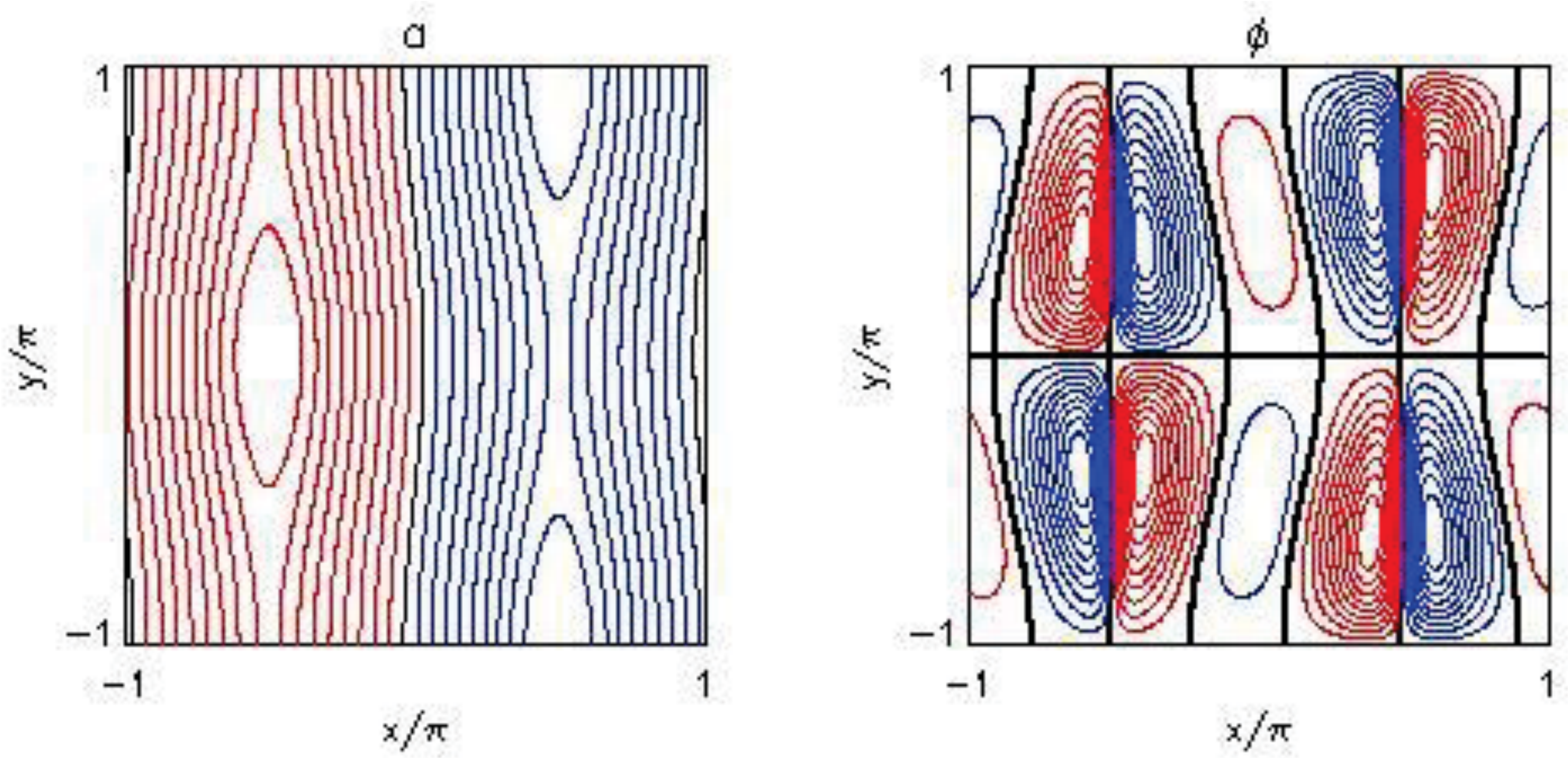

- When the Hall effect is neglected (pure MHD) **2D** reconnection is possible.

- Magnetic **fieldlines** (left) and flow **streamlines** (right) are shown at three succesive Alfven times. **Blue** contours are **positive** and the **red** ones are **negative**.

Hall-MHD reconnection in 2D

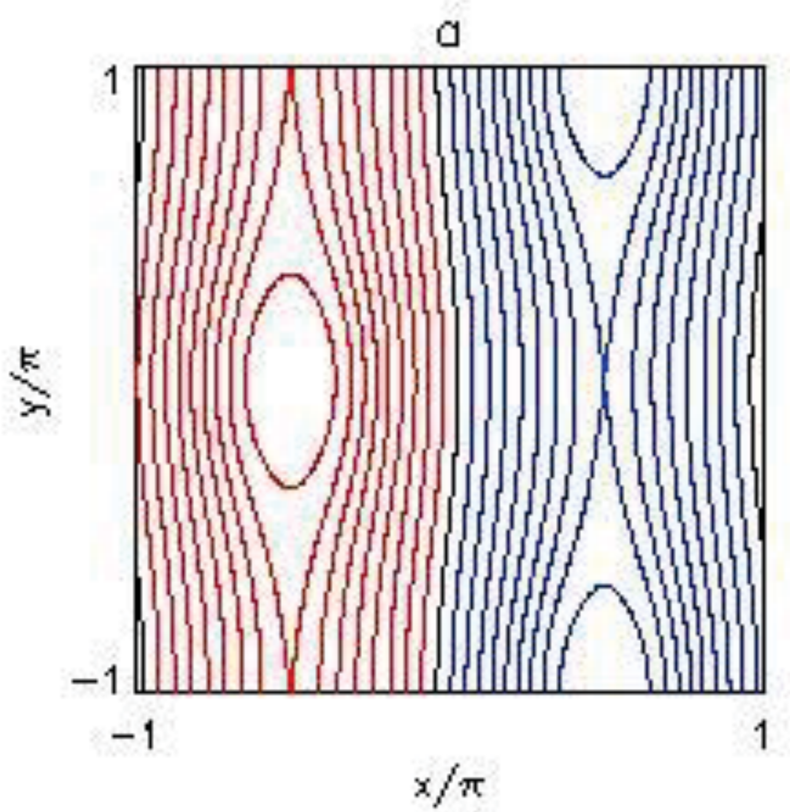

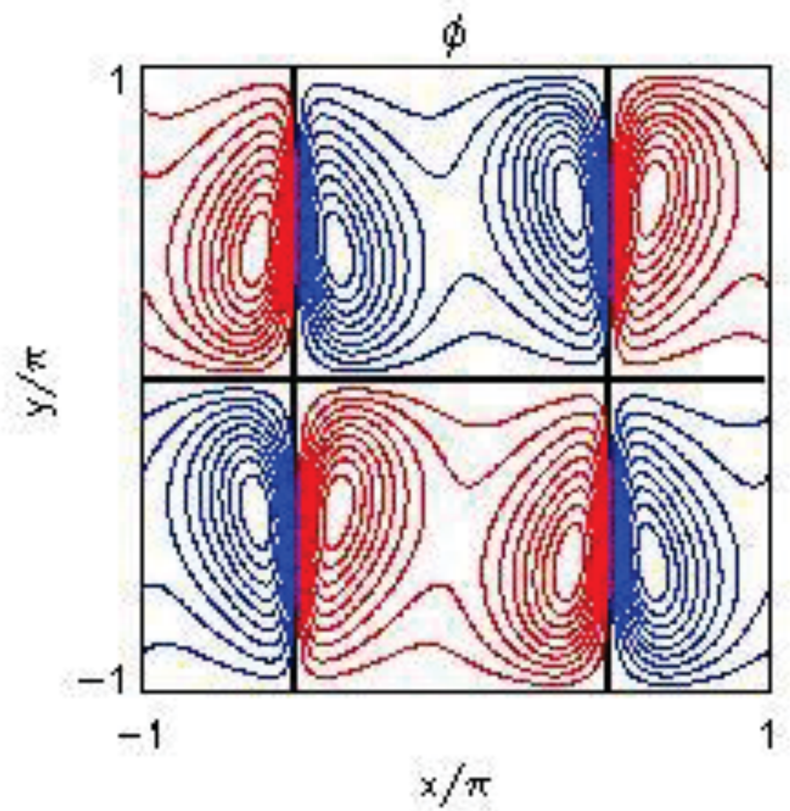

- When the Hall effect is neglected (pure MHD) **2D** reconnection is possible.

- Magnetic **fieldlines** (left) and flow **streamlines** (right) are shown at three succesive Alfven times. **Blue** contours are **positive** and the **red** ones are **negative**.

Hall-MHD reconnection in 2.5D

- When the Hall effect is considered, the out-of-plane fields are generated. They were initially set to zero.
- We show contour plots of the four scalar fields at three succesive Alfven times for $\varepsilon = 0.07$
- The out-of-plane magnetic field develops a quadrupolar pattern, while the velocity field develops a net flow at the reconnection region.
- **Blue** contours are **positive** and the **red** ones are **negative**.

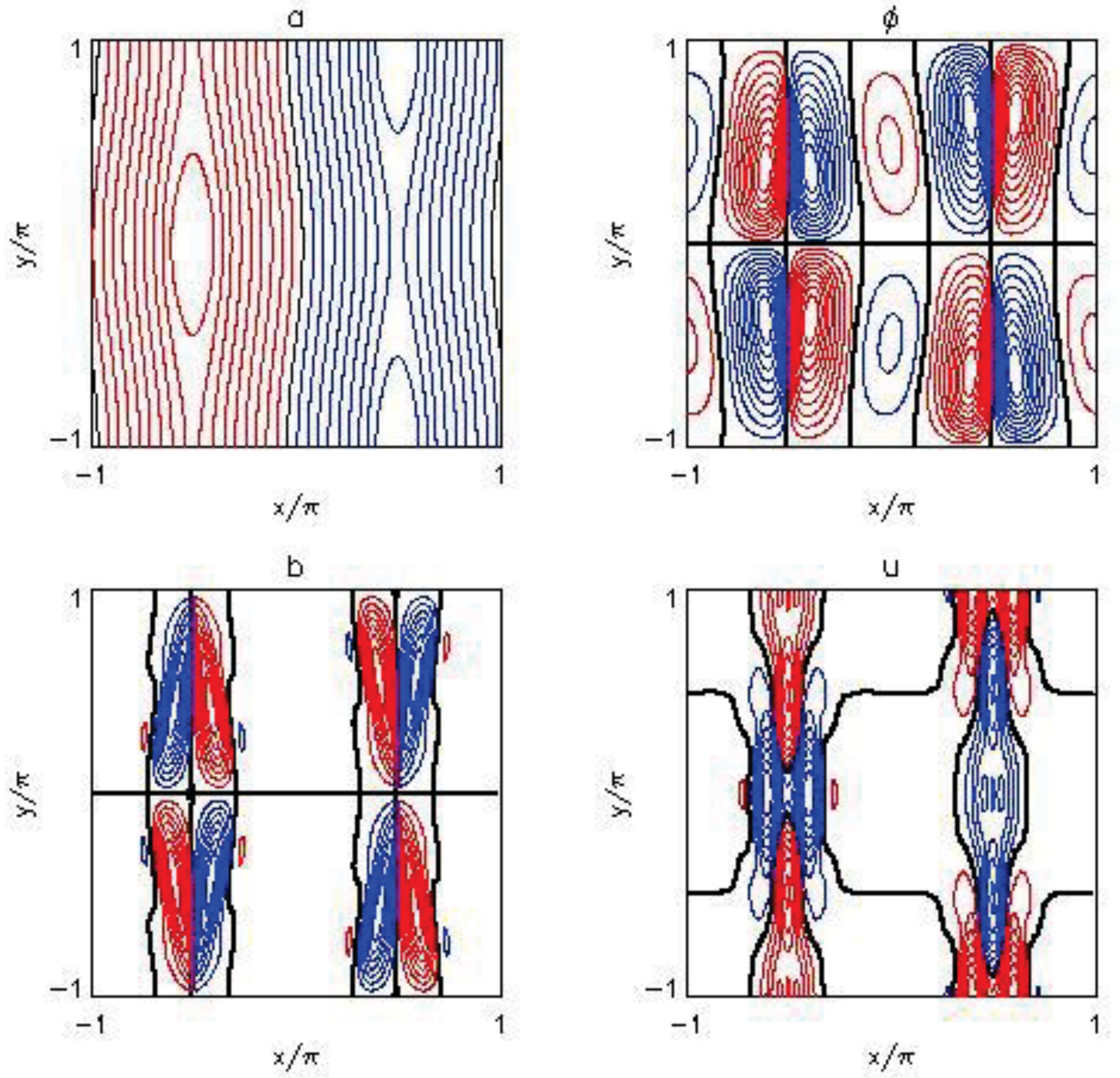

Hall-MHD reconnection in 2.5D

- When the Hall effect is considered, the out-of-plane fields are generated. They were initially set to zero.
- We show contour plots of the four scalar fields at three succesive Alfven times for $\varepsilon = 0.07$
- The out-of-plane magnetic field develops a quadrupolar pattern, while the velocity field develops a net flow at the reconnection region.
- **Blue** contours are **positive** and the **red** ones are **negative**.

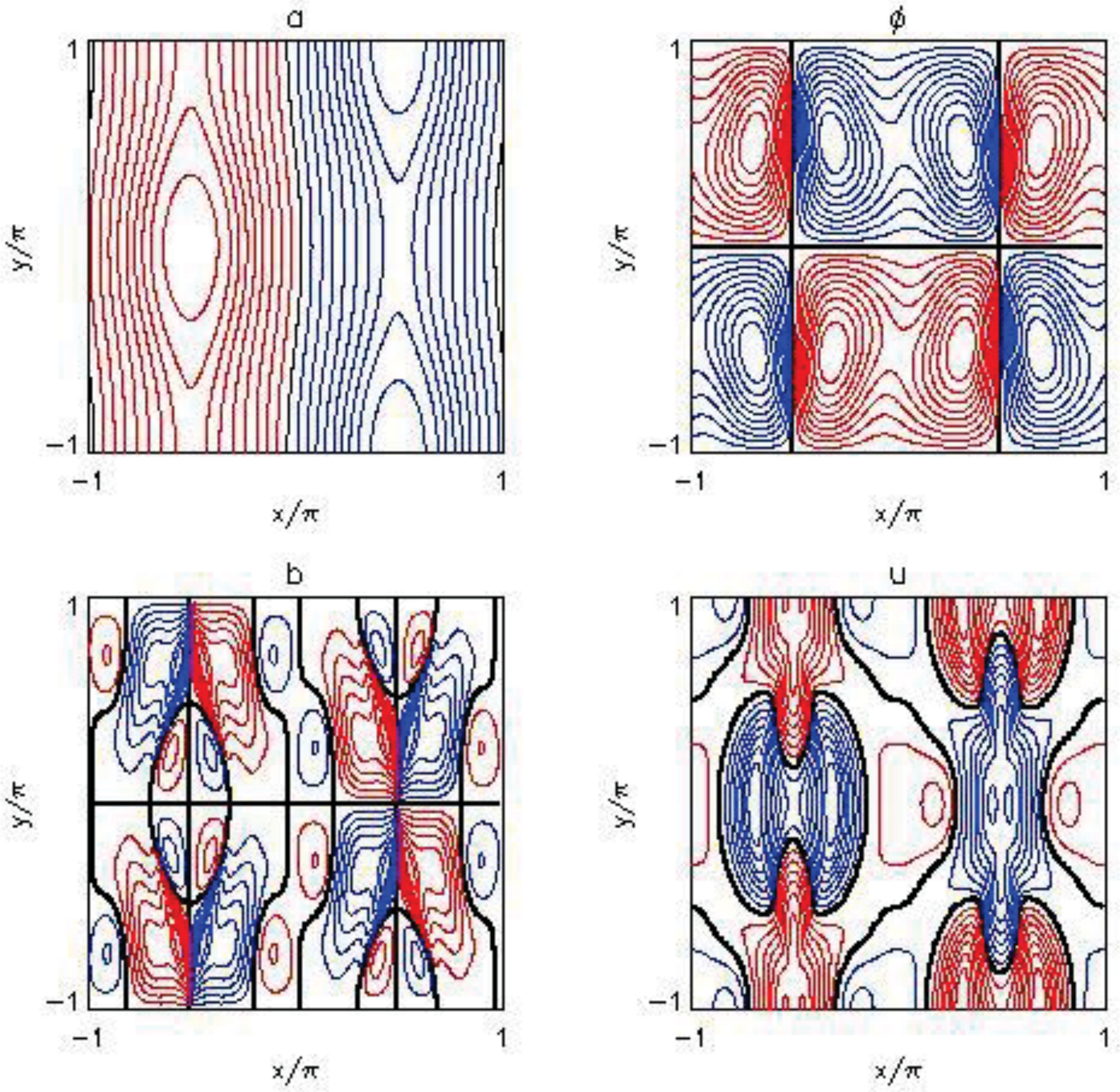

Hall-MHD reconnection in 2.5D

- When the Hall effect is considered, the out-of-plane fields are generated. They were initially set to zero.
- We show contour plots of the four scalar fields at three succesive Alfven times for $\varepsilon = 0.07$
- The out-of-plane magnetic field develops a quadrupolar pattern, while the velocity field develops a net flow at the reconnection region.
- **Blue** contours are **positive** and the **red** ones are **negative**.

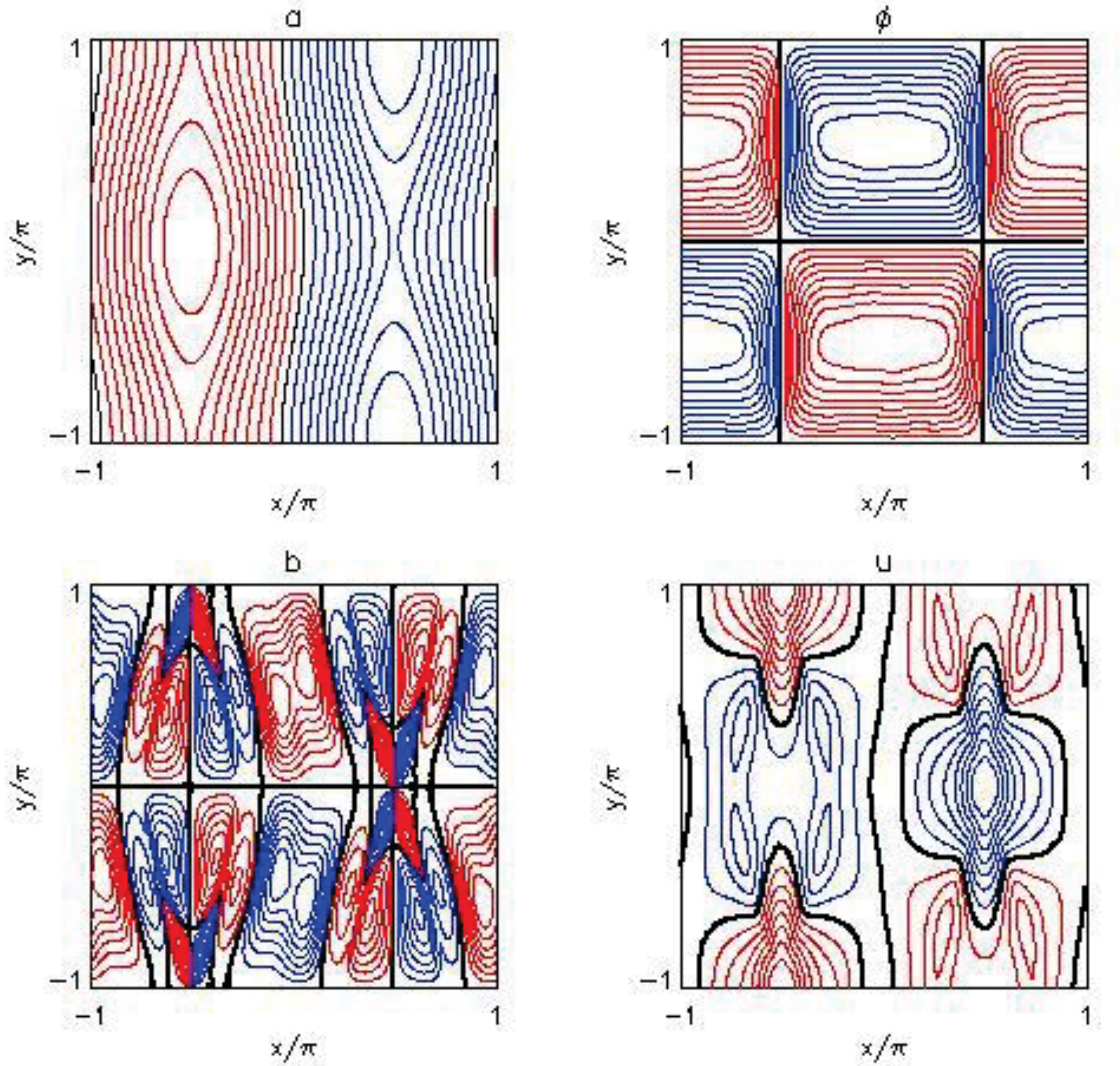

Hall-MHD reconnection rates

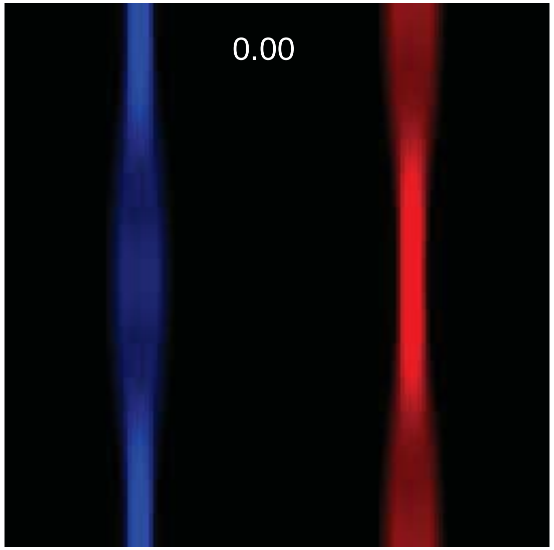

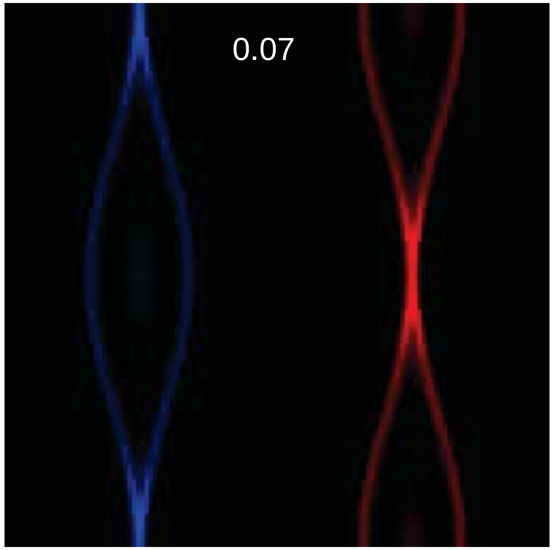

- The out-of-plane **current density** is shown for the cases $\varepsilon = 0.00$ *and* 0.07
- The current sheets becomes narrower and smaller as the Hall parameter is increased.
- The **reconnected flux** also increases with the Hall parameter, confirming previous results from collisionless and also Hall-MHD simulations.
- The plot shows reconnected flux vs. time for different values of the Hall parameter.

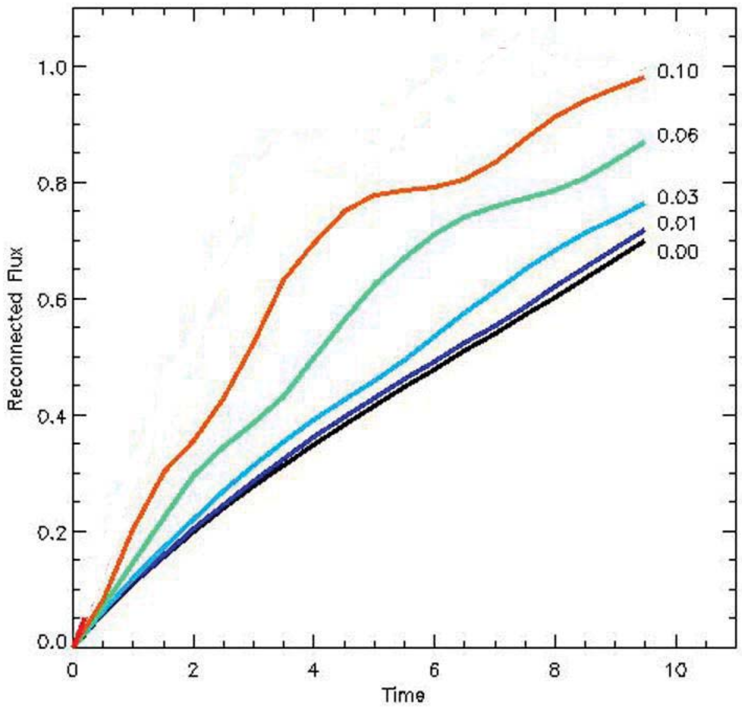

Energy spectra

- We also computed energy power spectra for different values of the Hall parameter ε.
- The Kolmogorov slope $k^{-5/3}$ is also displayed for reference.
- The dotted curves correspond to the parallel energy spectra.
- The vertical dotted lines indicate the location of the Hall scale $k_\varepsilon \cong 1/\varepsilon$ for each run.

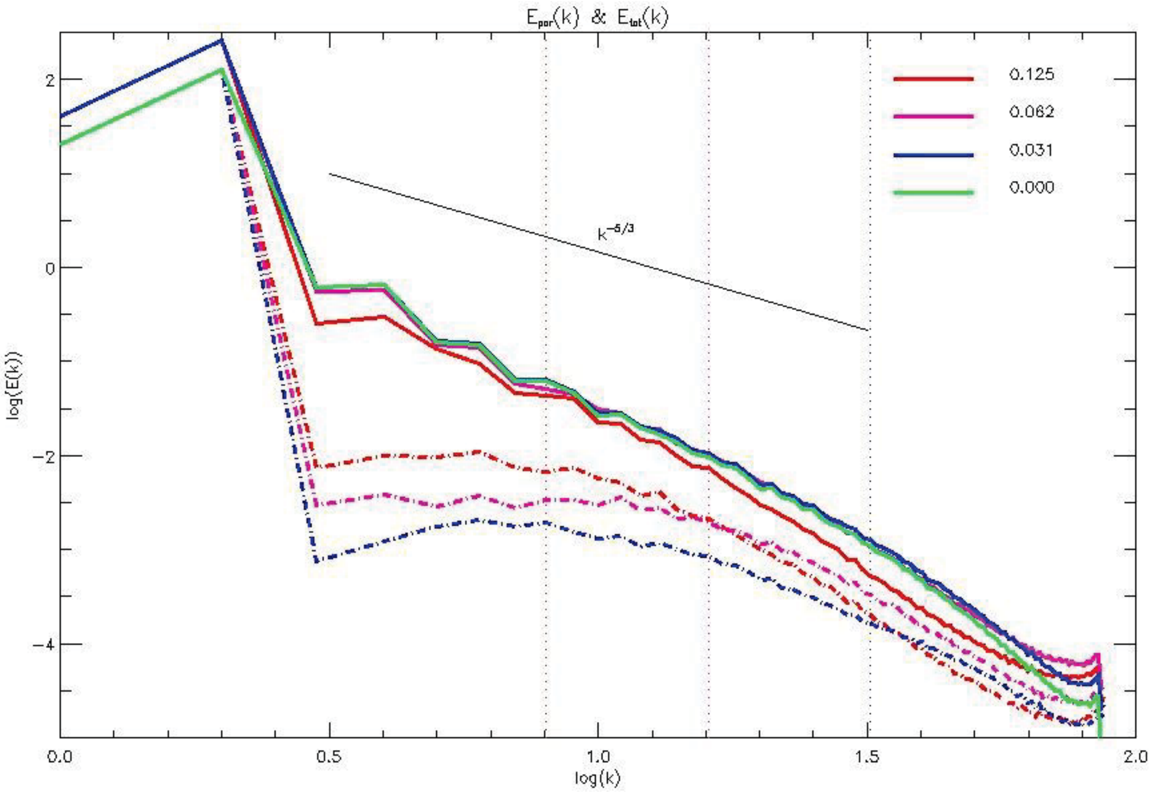

Energy spectra

- Energy power spectra for different values of ε.
- The dotted curves are the spectra for kinetic energy.

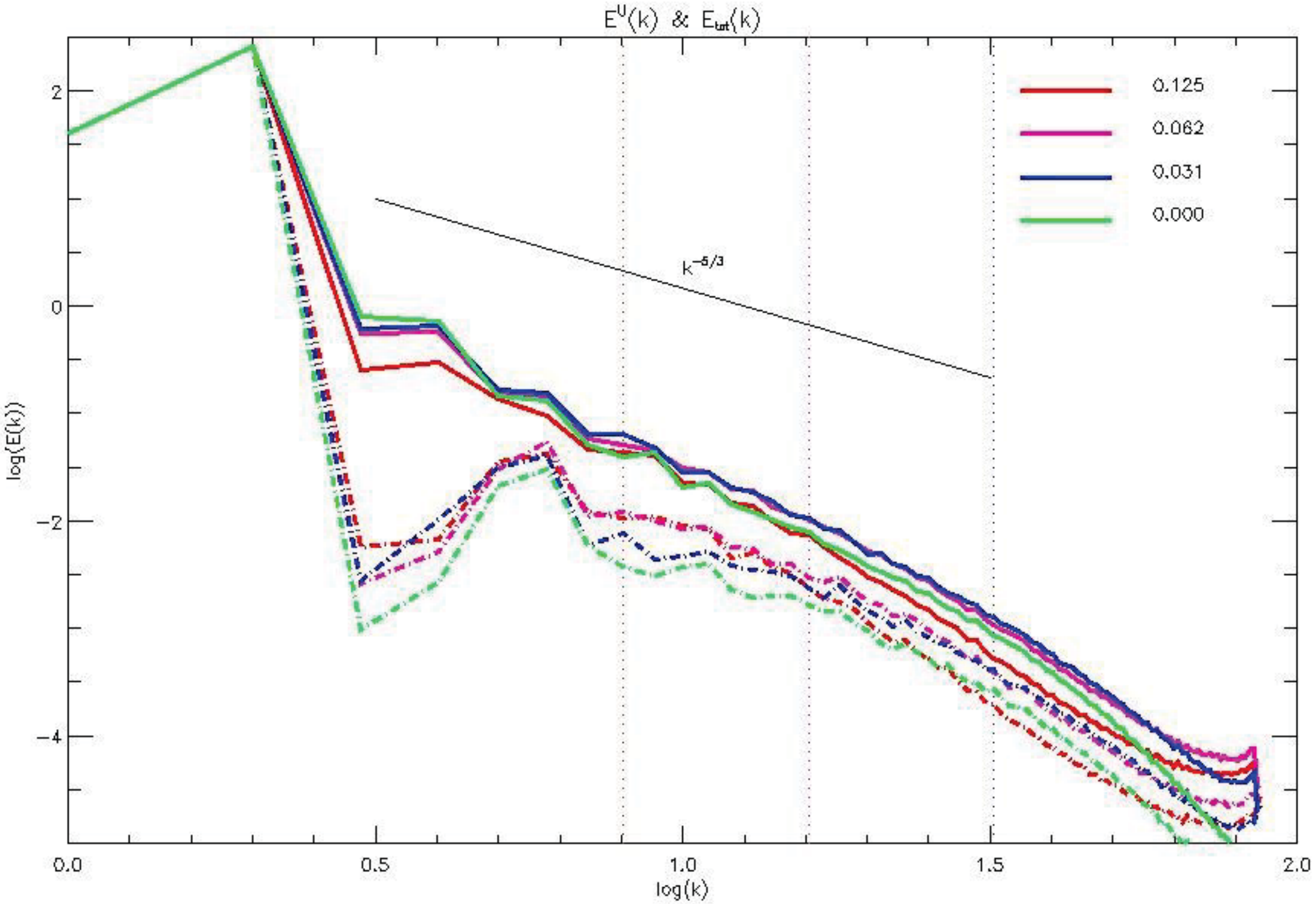

Current sheets in RHMHD

- Energy dissipation concentrates on very small structures known as current sheets, in which current density flows almost parallel to z.
- The picture shows **positive** and **negative** current density in a transverse cut at $z=\frac{1}{2}$, for pure RMHD (i.e. $\varepsilon=0$).
- When the Hall effect is considered, current sheets display the typical Petschek-like structure.

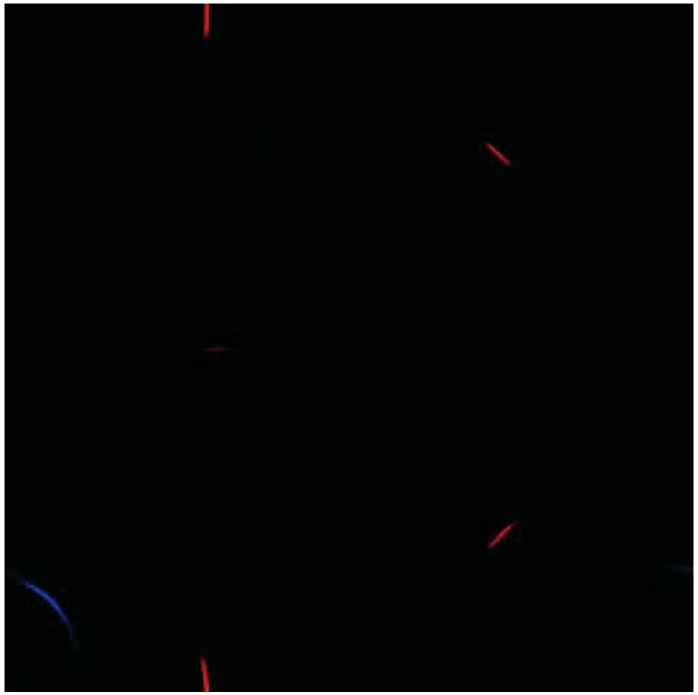

$\varepsilon=0.0$

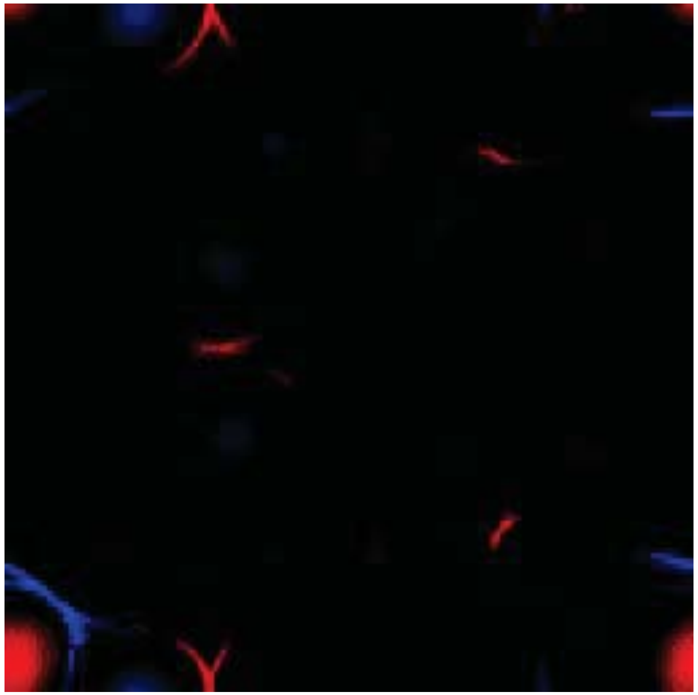

$\varepsilon=0.1$

Parallel electric field

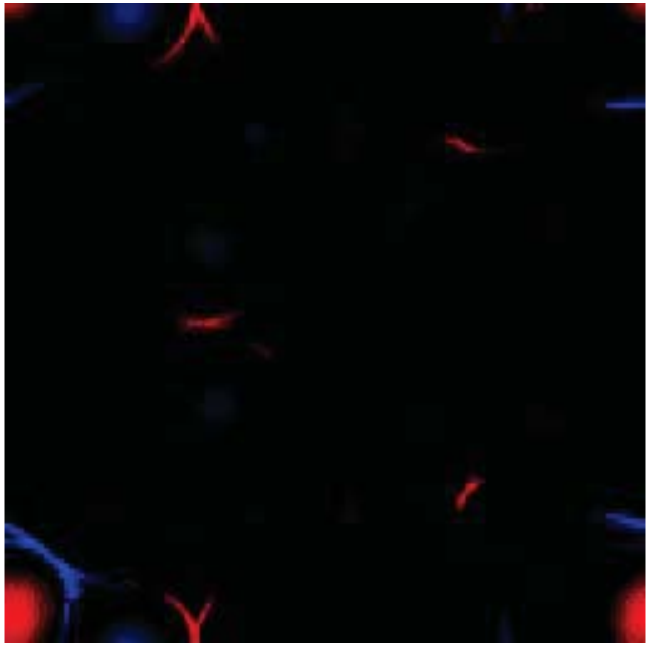

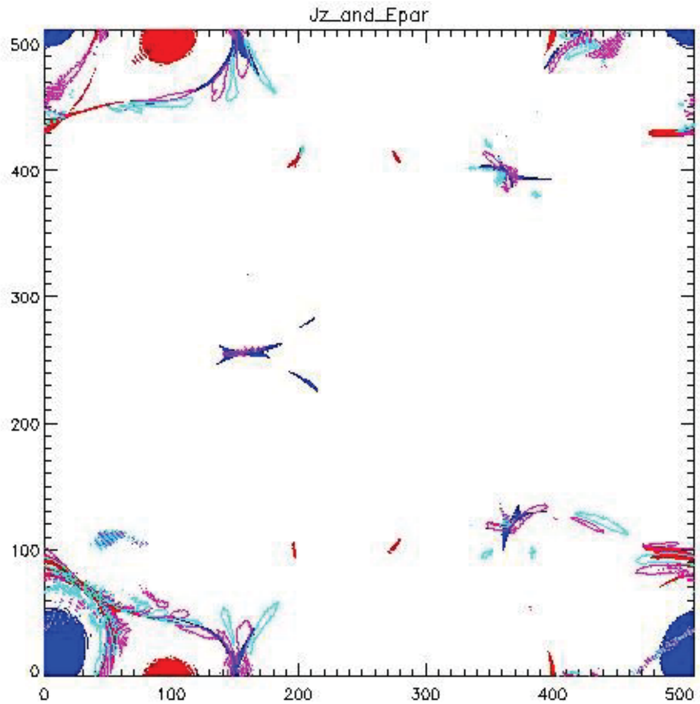

- One of the important new features of the Hall effect, is the presence of a parallel electric field, i.e. $E_{//} = \dfrac{\vec{E} \cdot \vec{B}}{|\vec{B}|}$
- To order α^2 it can be computed as $\boxed{E_{//} = \varepsilon(\partial_z b - [a, b])}$

  and of course it can potentially accelerate particles along magnetic field lines.
- Current density is displayed in **red** and **blue**, while contours coloured in **light blue** and **pink** correspond to the parallel electric field.

… back to multi-species plasmas

- For each species s we have (Goldston & Rutherford 1995):
  - Mass conservation $$\frac{\partial n_s}{\partial t} + \vec{\nabla} \cdot (n_s \vec{U}_s) = 0$$
  - Equation of motion $$m_s n_s \frac{d\vec{U}_s}{dt} = q_s n_s (\vec{E} + \frac{1}{c}\vec{U}_s \times \vec{B}) - \vec{\nabla} p_s + \vec{\nabla} \bullet \overleftrightarrow{\sigma}_s + \sum_{s'} \vec{R}_{ss'}$$
  - Momentum exchange rate $$\vec{R}_{ss'} = -m_s n_s \upsilon_{ss'} (\vec{U}_s - \vec{U}_{s'})$$

- These moving charges act as sources for electric and magnetic fields:
  - Charge density $$\rho_c = \sum_s q_s n_s \approx 0$$
  - Electric current density $$\vec{J} = \frac{c}{4\pi} \vec{\nabla} \times \vec{B} = \sum_s q_s n_s \vec{U}_s$$

Two-fluid MHD equations

- Let us now retain electron inertia (i.e. $0 < m_e << m_i$):

  - Mass conservation: $$0 = \frac{\partial n}{\partial t} + \vec{\nabla} \cdot (n\vec{U}) \quad , \qquad n_e \cong n_i \cong n$$
  - Ions: $$m_i n \frac{d\vec{U}}{dt} = en(\vec{E} + \frac{1}{c}\vec{U} \times \vec{B}) - \vec{\nabla} p_i + \vec{R}$$
  - Electrons: $$m_e n \frac{d\vec{U}_e}{dt} = -en(\vec{E} + \frac{1}{c}\vec{U}_e \times \vec{B}) - \vec{\nabla} p_e - \vec{R}$$
  - Friction force: $$\vec{R} = -m_i n \nu_{ie} (\vec{U} - \vec{U}_e)$$
  - Ampere's law: $$\vec{J} = \frac{c}{4\pi} \vec{\nabla} \times \vec{B} = en(\vec{U} - \vec{U}_e) \quad \Rightarrow \quad \vec{R} = -\frac{m\upsilon_{ie}}{e} \vec{J}$$
  - Polytropic laws: $$p_i \propto n^\gamma \quad , \qquad p_e \propto n^\gamma$$

Retaining electron inertia: EIHMHD equations

- The dimensionless version, for a length scale L_0, density n_0 and Alfven speed $V_A = B_0 / \sqrt{4\pi m_i n_0}$

$$\frac{d\vec{U}_i}{dt} = \frac{1}{\varepsilon}(\vec{E} + \vec{U}_i \times \vec{B}) - \frac{\beta}{n}\vec{\nabla} p_i - \frac{\eta}{\varepsilon n}\vec{J}$$

$$\frac{m_e}{m_i}\frac{d\vec{U}_e}{dt} = -\frac{1}{\varepsilon}(\vec{E} + \vec{U}_e \times \vec{B}) - \frac{\beta}{n}\vec{\nabla} p_e + \frac{\eta}{\varepsilon n}\vec{J}$$

where $\vec{J} = \vec{\nabla} \times \vec{B} = \frac{n}{\varepsilon}(\vec{U}_i - \vec{U}_e)$

- We defined the Hall parameter $\varepsilon = \frac{c}{\omega_{pi} L_0}$

  as well as the plasma *beta* $\beta = \frac{p_0}{m_i n_0 V_A^2}$ and the electric resistivity $\eta = \frac{c^2 \nu_{ie}}{\omega_{pi}^2 L_0 V_A}$

- Adding these two equations yields:

$$\boxed{n\frac{d\vec{U}}{dt} = (\vec{\nabla} \times \vec{B}) \times \vec{B} - \beta\vec{\nabla} p}$$

where $\vec{U} = \frac{m_i \vec{U}_i + m_e \vec{U}_e}{m_i + m_e}$

and $p = p_i + p_e$

Retaining electron inertia: EIHMHD equations

- In the equation for electrons (assuming incompressibility)

$$\frac{m_e}{m_i}\frac{d\vec{U}_e}{dt} = -\frac{1}{\varepsilon}(\vec{E}+\vec{U}_e\times\vec{B}) - \beta_e\vec{\nabla}p_e + \frac{\eta}{\varepsilon}\vec{J} \qquad \vec{J}=\vec{\nabla}\times\vec{B}=\frac{1}{\varepsilon}(\vec{U}_i-\vec{U}_e)$$

we replace $\quad \vec{E}=-\frac{1}{c}\frac{\partial\vec{A}}{\partial t}-\vec{\nabla}\phi \quad and \quad \vec{B}=\vec{\nabla}\times\vec{A}$

to obtain

$$\boxed{\frac{\partial}{\partial t}(\vec{A}-\varepsilon_e^2\nabla^2\vec{A}-\frac{\varepsilon_e^2}{\varepsilon}\vec{U})=(\vec{U}-\varepsilon\vec{J})\times(\vec{B}-\varepsilon_e^2\nabla^2\vec{B}-\frac{\varepsilon_e^2}{\varepsilon}\vec{W})-\vec{\nabla}(\phi-\varepsilon\beta_e p_e-\frac{\varepsilon_e^2}{\varepsilon}\frac{U_e^2}{2})+\eta\nabla^2\vec{A}}$$

- Electron inertia is quantified by the dimensionless parameter $\varepsilon_e = \sqrt{\frac{m_e}{m_i}}\,\varepsilon = \frac{c}{\omega_{pe}L_0}$

- Just as the Hall effect introduces the new spatial scale $k_H = \frac{1}{\varepsilon}$ (the ion skin depth), electron inertia introduces the electron skin depth $k_e = \frac{1}{\varepsilon_e}$ which satisfies

$$k_e = \sqrt{\frac{m_i}{m_e}}\,k_H >> k_H$$

EIHMHD in 2.5D

- We now express the EIHMHD equations in 2.5D geometry. I.e. for simplicity we assume $\partial_z = 0$ and therefore

$$\vec{B} = \vec{\nabla} \times \left[\hat{z}\, a(x, y, t)\right] + \hat{z}\, b(x, y, t)$$
$$\vec{U} = \vec{\nabla} \times \left[\hat{z}\varphi(x, y, t)\right] + \hat{z}\, u(x, y, t)$$

- The equations for these four scalar fields are

$$\boxed{\begin{aligned}
\partial_t a' &= [\varphi - \varepsilon b, a'] && + \eta \nabla_\perp^2 a \\
\partial_t \omega &= [\varphi, \omega] - [a, j] && + \nu \nabla_\perp^2 \omega \\
\partial_t b' &= [\varphi - \varepsilon b, b'] + [u - \varepsilon j, a'] && + \eta \nabla_\perp^2 b \\
\partial_t u &= [\varphi, u] - [a, b] && + \nu \nabla_\perp^2 u
\end{aligned}}$$

where

$$a' = (1 - \varepsilon_e^2 \nabla_\perp^2) a - \frac{\varepsilon_e^2}{\varepsilon} u \qquad and \qquad b' = (1 - \varepsilon_e^2 \nabla_\perp^2) b - \frac{\varepsilon_e^2}{\varepsilon} w$$

Normal modes in EIHMHD

- If we linearize our equations around an equilibrium characterized by a uniform magnetic field, we obtain the following dispersion relation:

$$\left(\frac{\omega}{\vec{k}\bullet\vec{B}_0}\right)^2 \pm \frac{k\varepsilon}{1+\varepsilon_e^2 k^2}\left(\frac{\omega}{\vec{k}\bullet\vec{B}_0}\right) - \frac{1}{1+\varepsilon_e^2 k^2} = 0$$

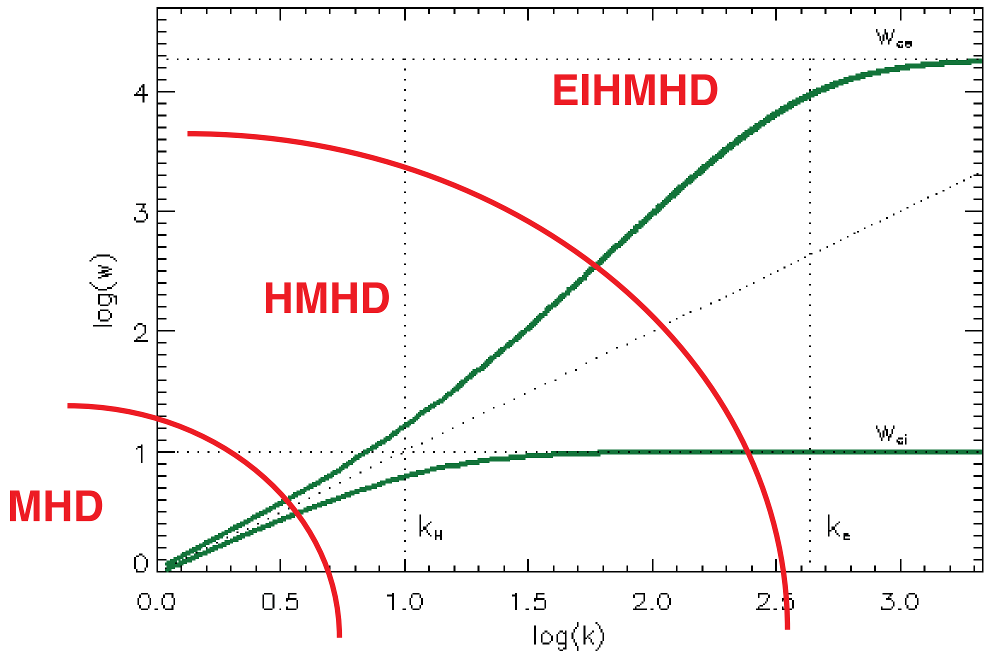

- Asymptotically, at very large k, we have two branches

$$\omega \xrightarrow[k\to\infty]{} \omega_{ce}\cos\theta$$

$$\omega \xrightarrow[k\to\infty]{} \omega_{ci}\cos\theta$$

while for very small k, both branches simply become Alfven modes, i.e.

$$\omega \xrightarrow[k\to 0]{} k\cos\theta$$

- Different approximations, just as one-fluid MHD, Hall-MHD and electron-inertia HMHD can clearly be identified in this diagram.

Ideal invariants in EIHMHD

- For each species s in the incompressible and ideal limit

$$m_s n_s\left(\partial_t \vec{U}_s - \vec{U}_s \times \vec{W}_s\right) = q_s n_s\left(\vec{E} + \frac{1}{c}\vec{U}_s \times \vec{B}\right) - \vec{\nabla}\left(p_s + m_s n_s \frac{U_s^2}{2}\right)$$

- Using that $\vec{J} = \frac{c}{4\pi}\vec{\nabla}\times\vec{B} = \sum_s q_s n_s \vec{U}_s$ and $E = -\frac{1}{c}\partial_t \vec{A} - \vec{\nabla}\phi$

  we can readily show that energy is an ideal invariant, where

$$E = \int d^3 r \left(\sum_s m_s n_s \frac{U_s^2}{2} + \frac{B^2}{8\Pi}\right)$$

- We also have a helicity per species which is conserved, where

$$H_s = \int d^3 r \left(\vec{A} + \frac{c m_s}{q_s}\vec{U}_s\right) \bullet \left(\vec{B} + \frac{c m_s}{q_s}\vec{W}_s\right)$$

EIHMHD simulations

- We perform 512x512 simulations of the EIHMHD equations in 2.5D geometry to study magnetic reconnection.
- We force an external field with a double hyperbolic tangent profile to drive reconnection at two X points.
- At three succesive times we show the current density in the background, the proton flow in the left half of each frame, and the electron flow on the right half.
- Although at large scales both flows look quite similar, in the vecinity of the X points, electrons tend to move much faster, close to the Alfven velocity.

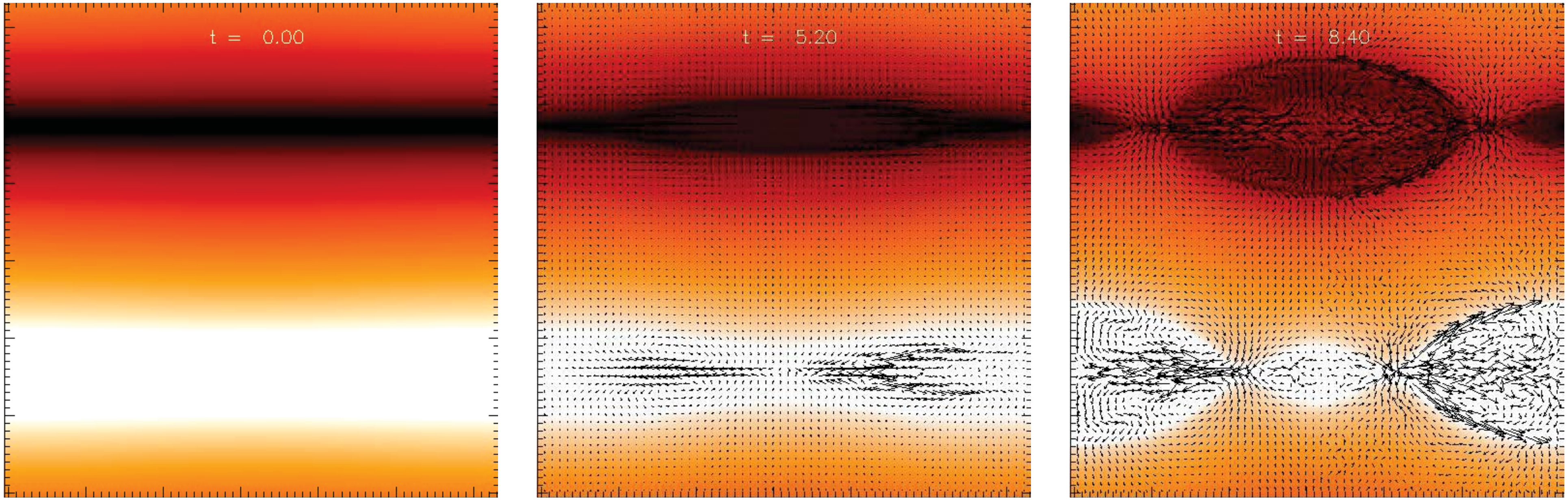

Reconnected flux in EIHMHD

- The total reconnected flux at the X-point is the magnetic flux through the perpendicular surface that extends from the O-point to the X-point.

- We compare the total reconnected flux between a run that includes electron inertia and another one that does not.

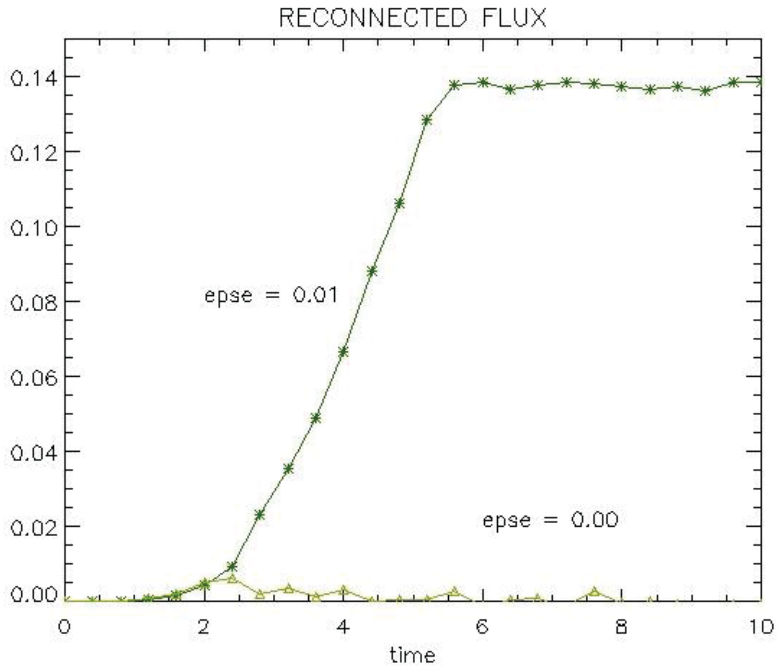

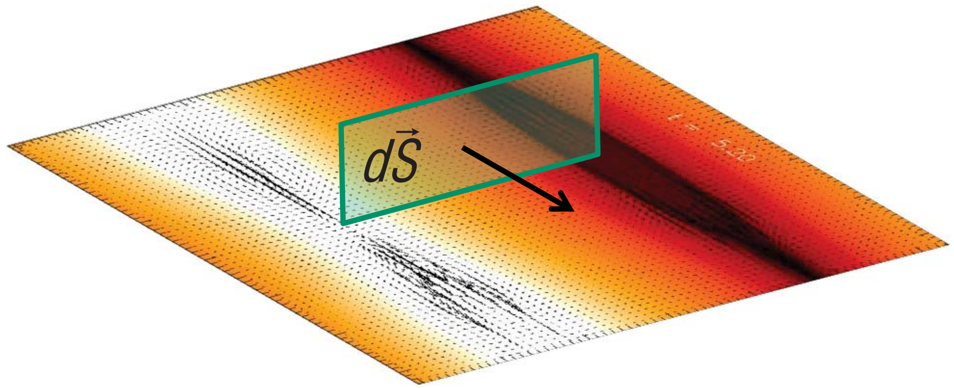

- The reconnection rate is the time derivative of these two curves.

- The apparent saturation is just a spurious effect stemming from the dynamical destruction of the X-point.

Conclusions

- In this presentation, we integrated the Hall-MHD equations numerically, to study magnetic reconnection. Even though the Hall effect does not produce reconnection, its role is to enhance the Ohmic reconnection rate.

- We also studied the role of the Hall effect in the presence of a strong external magnetic field. We showed the development of Kolmogorov-like turbulence in this system. Also, the existence of parallel electric fields can provide particle acceleration.

- We extended the Hall-MHD equations to include electron inertia, leading to what we call the EIHMHD equations.

- Integrating the EIHMHD equations in a 2.5D setup, we show that electron inertia leads to efficient magnetic reconnection, even in the absence of magnetic resistivity.

- The ideal invariants of a multi-species plasma are the total energy and also one helicity per species.